

**Myocardial blood flow reserve is impaired in patients with aortic valve calcification and unobstructed epicardial coronary arteries**

Author

Nel, Karen, Nam, Michael CY, Anstey, Chris, Boos, Christopher J, Carlton, Edward, Senior, Roxy, Kaski, Juan Carlos, Khattab, Ahmed, Shamley, Delva, Byrne, Christopher D, Stanton, Tony, Greaves, Kim

Published

2017

Journal Title

International Journal of Cardiology

Version

Accepted Manuscript (AM)

DOI

[10.1016/j.ijcard.2017.06.023](https://doi.org/10.1016/j.ijcard.2017.06.023)

Rights statement

© 2017 Elsevier. Licensed under the Creative Commons Attribution-NonCommercial-NoDerivatives 4.0 International Licence (<http://creativecommons.org/licenses/by-nc-nd/4.0/>) which permits unrestricted, non-commercial use, distribution and reproduction in any medium, providing that the work is properly cited.

Downloaded from

<http://hdl.handle.net/10072/387558>

Griffith Research Online

<https://research-repository.griffith.edu.au>

1  
2  
3 **Title: Myocardial Blood Flow Reserve Is Impaired In Patients With Aortic Valve Calcification And**  
4  
5 **Unobstructed Epicardial Coronary Arteries**  
6  
7

8  
9 Karen Nel<sup>1</sup>, Michael C Y Nam<sup>2</sup>, Chris Anstey<sup>3</sup>, Christopher J Boos<sup>4</sup>, Edward Carlton<sup>5</sup>, Roxy Senior<sup>6</sup>, Juan Carlos  
10 Kaski<sup>7</sup>, Ahmed Khattab<sup>8</sup>, Delva Shamley<sup>9</sup>, Christopher Byrne<sup>10</sup>, Kim Greaves<sup>11</sup>  
11

12  
13  
14 <sup>1</sup>Department of Cardiology, Poole Hospital NHS Foundation Trust, Centre for Postgraduate Medical Research  
15 and Education, Bournemouth University, Dorset, UK. *This author takes responsibility for all aspects of the*  
16 *reliability and freedom from bias of the data presented and their discussed interpretation*  
17  
18

19  
20 <sup>2</sup>Department of Cardiology, Sunshine Coast Hospital and Health Services, University of the Sunshine Coast and  
21 University of Queensland, Queensland, Australia. *This author takes responsibility for all aspects of the reliability*  
22 *and freedom from bias of the data presented and their discussed interpretation*  
23  
24

25  
26 <sup>3</sup>Department of Intensive Care, Sunshine Coast Hospital and Health Services and University of Queensland,  
27 Queensland, Australia. *This author takes responsibility for all aspects of the reliability and freedom from bias of*  
28 *the data presented and their discussed interpretation*  
29  
30

31  
32 <sup>4</sup>Department of Cardiology, Poole Hospital NHS Foundation Trust, Centre for Postgraduate Medical Research  
33 and Education, Bournemouth University, Dorset, UK. *This author takes responsibility for all aspects of the*  
34 *reliability and freedom from bias of the data presented and their discussed interpretation*  
35  
36

37  
38 <sup>5</sup>Department of Cardiology, Poole Hospital NHS Foundation Trust, Centre for Postgraduate Medical Research  
39 and Education, Bournemouth University, Dorset, UK. *This author takes responsibility for all aspects of the*  
40 *reliability and freedom from bias of the data presented and their discussed interpretation*  
41  
42

43  
44 <sup>6</sup>Biomedical Research Unit, National Heart and Lung Institute, Imperial College, London, Royal Brompton  
45 Hospital, London, UK. *This author takes responsibility for all aspects of the reliability and freedom from bias of*  
46 *the data presented and their discussed interpretation*  
47  
48

49  
50 <sup>7</sup>Cardiovascular Science Research Centre, St George's Healthcare Trust, London, UK. *This author takes*  
51 *responsibility for all aspects of the reliability and freedom from bias of the data presented and their discussed*  
52 *interpretation*  
53  
54  
55  
56  
57  
58  
59  
60

61  
62  
63 <sup>8</sup>Centre for Postgraduate Medical Research and Education, Bournemouth University, Dorset, UK. *This author*  
64 *takes responsibility for all aspects of the reliability and freedom from bias of the data presented and their*  
65 *discussed interpretation*  
66  
67

68  
69 <sup>9</sup>Centre for Postgraduate Medical Research and Education, Bournemouth University, Dorset, UK. *This author*  
70 *takes responsibility for all aspects of the reliability and freedom from bias of the data presented and their*  
71 *discussed interpretation*  
72  
73

74 <sup>10</sup>Nutrition & Metabolism, Institute for Developmental Sciences, University of Southampton and Southampton  
75 National Institute for Health Research Biomedical Research Centre, University Hospital Southampton,  
76 Southampton General Hospital, Southampton, UK. *This author takes responsibility for all aspects of the*  
77 *reliability and freedom from bias of the data presented and their discussed interpretation*  
78  
79

80  
81 <sup>11</sup>Department of Cardiology, Sunshine Coast Hospital and Health Services, University of the Sunshine Coast and  
82 University of Queensland, Queensland, Australia *This author takes responsibility for all aspects of the reliability*  
83 *and freedom from bias of the data presented and their discussed interpretation*  
84  
85  
86  
87

88  
89  
90  
91 **Correspondence author:**

92 Professor Kim Greaves

93 Department of Cardiology

94 Sunshine Coast Hospital and Health Services

95 Nambour 4565, Queensland, Australia.

96 Email: kim.greaves@health.qld.gov.au

97 Tel: +61 7 5370 3727

98 Fax: +61 7 5470 6084

99  
100  
101  
102  
103  
104  
105  
106  
107  
108 **Grant support:** Bournemouth University PhD Scholarship, The Dorset Research Consortium and the Poole  
109 Hospital Cardiology Research Fund

110  
111 **Conflicts of interest:** None to declare

112  
113  
114 **Keywords:** Aortic valve calcification score, coronary microvascular dysfunction, calcific aortic valve disease.  
115  
116  
117  
118  
119  
120

121  
122  
123 **Abstract:**  
124

125 **Background:** Although calcific aortic valve disease (CAVD) is associated with coronary atherosclerosis, it is not  
126 known whether early CAVD is associated with coronary microcirculatory dysfunction (CMD). We sought to  
127 investigate the relationship between myocardial blood flow reserve (MBFR) - a measure of CMD, and early  
128 CAVD. We also determined whether this relationship was independent of coronary artery disease (CAD) and hs-  
129 CRP, a marker of systemic inflammation.  
130  
131  
132  
133

134 **Methods:** 183 patients with chest pain and unobstructed coronary arteries were studied. Aortic valve  
135 calcification score (AVCS), coronary total plaque length (TPL), and coronary calcium score were quantified from  
136 multislice CT. MBFR was assessed using vasodilator myocardial contrast echocardiography. Hs-CRP was  
137 measured from venous blood using a particle-enhanced immunoassay.  
138  
139  
140  
141

142 **Results:** Mean( $\pm$ SD) participant age was 59.8(9.6) years. Mean AVCS was 68(258) AU, TPL was 15.6(22.2) mm,  
143 and median coronary calcification score was 43.5AU. Mean MBFR was 2.20(0.52). Mean hs-CRP was 2.52(3.86)  
144 mg/L. Multivariable linear regression modelling incorporating demographics, coronary plaque characteristics,  
145 MBFR, and inflammatory markers, demonstrated that age ( $\beta=0.05$ , 95%CI:0.02,0.08,  $P=0.007$ ), hs-CRP ( $\beta=0.09$ ,  
146 CI:0.02,0.16,  $P=0.010$ ) and diabetes ( $\beta=1.03$ , CI:0.08,1.98,  $P=0.033$ ), were positively associated with AVCS.  
147  
148  
149  
150  
151  
152  
153  
154  
155  
156  
157  
158  
159  
160  
161  
162  
163  
164  
165  
166  
167  
168  
169  
170  
171  
172  
173  
174  
175  
176  
177  
178  
179  
180

151 MBFR ( $\beta=-0.87$ , CI:-1.44,-0.30,  $P=0.003$ ), BMI ( $\beta=-0.11$ , CI:-0.21,-0.01,  $P=0.033$ ), and LDL ( $\beta=-0.32$ , CI:-0.61,-  
152 0.03,  $P=0.029$ ) were negatively associated with AVCS. TPL and coronary calcium score were not independently  
153 associated with AVCS when included in the regression model.  
154  
155  
156  
157  
158  
159  
160  
161  
162  
163  
164  
165  
166  
167  
168  
169  
170  
171  
172  
173  
174  
175  
176  
177  
178  
179  
180

157 **Conclusion:** Coronary microvascular function as determined by measurement of myocardial blood flow reserve  
158 is an independent predictor of early CAVD. This effect is independent of the presence of coronary artery  
159 disease and also systemic inflammation.  
160  
161  
162  
163  
164  
165  
166  
167  
168  
169  
170  
171  
172  
173  
174  
175  
176  
177  
178  
179  
180

181  
182  
183 **1. Introduction:**  
184  
185  
186

187 The development of calcific aortic valve disease (CAVD) has traditionally been attributed to a passive, age-  
188 related degenerative phenomenon. However recent evidence suggests a more active mechanism. CT coronary  
189 angiographic studies have found an association between aortic valve calcification and the presence of coronary  
190 artery disease, which is an inflammatory process (1, 2). Epidemiologic studies have identified that risk factors  
191 for atherosclerosis - older age, male sex, hypercholesterolemia, hypertension, metabolic syndrome, and  
192 smoking, are also independently associated with the presence of CAVD (3). Histopathological studies have also  
193 observed the accumulation of atherosclerotic end products such as LDL, inflammatory cell infiltrates and  
194 microscopic calcification, within explanted or cadaveric CAVD specimens (4). In addition, more recent findings  
195 have shown that markers of inflammation such as hs-CRP, are independently associated with aortic valve  
196 calcification (5). In the light of these and other findings, several groups have suggested that CAVD and coronary  
197 atherosclerosis share common active pathophysiological mechanisms (6, 7).  
198  
199  
200  
201  
202  
203  
204  
205  
206  
207

208  
209 The discovery of a link between both the early CAVD and coronary atherosclerosis has the potential to increase  
210 understanding of the disease, improve risk stratification and provide therapeutic targets. Coronary  
211 microvascular dysfunction (CMD) is a precursor to the development of coronary atherosclerosis (8). The  
212 presence of CMD has been shown to predict the future development of coronary artery disease, and also  
213 independently predict adverse cardiovascular and all-cause mortality. Therapies to improve CMD and outcome  
214 have had some success (9-11). Whether or not CMD is independently associated with early CAVD is unknown.  
215 Previous studies have attempted to examine whether there is a direct link between CMD and CAVD. However,  
216 these have been limited to patients with established aortic stenosis which therefore represents late stage  
217 CAVD, or assessed CAVD with echocardiography rather than CT (12, 13). Furthermore these studies either did  
218 not exclude or quantify whether coronary artery disease was also present (14). This is important because even  
219 the presence of mild non-obstructive coronary artery disease is known to be independently associated with  
220 CMD and therefore a confounding factor (15)  
221  
222  
223  
224  
225  
226  
227  
228  
229  
230  
231  
232  
233  
234  
235  
236  
237  
238  
239  
240

241  
242  
243 We sought to investigate the relationship between myocardial blood flow reserve (MBFR) - a measure of CMD,  
244  
245 and early CAVD. We also determined whether this relationship was independent of coronary artery disease  
246  
247 (CAD) and hs-CRP, a marker of systemic inflammation.  
248  
249  
250  
251

## 252 **2. Methods:**

253  
254  
255  
256 **2.1. Study population:** This pre-determined study was part of another study investigating the relationship  
257  
258 between chest pain typicality and its relationship to coronary microvascular function. This was a prospective,  
259  
260 cross-sectional, observational study which recruited consecutive patients aged 30-80 years attending  
261  
262 cardiology outpatient clinics (Jan 2011-March 2013) presenting with stable chest pain suggestive of myocardial  
263  
264 ischaemia due to CAD and who were referred for diagnostic CT coronary angiography (CTA). Those with  
265  
266 unobstructed coronary arteries underwent transthoracic echocardiography. Unobstructed CAD was defined as  
267  
268 a quantitatively measured luminal diameter stenosis <50%. Patients were excluded if they had ≥50% luminal  
269  
270 diameter narrowing, known ischemic heart disease, left ventricular hypertrophy, an ejection fraction <55%, or  
271  
272 significant aortic valve disease. Specifically, those patients with a peak systolic transaortic valve velocity of  
273  
274 >2m/s were excluded. Aortic valve calcification was quantified from the CTCA study. Participants then  
275  
276 underwent vasodilator myocardial contrast echocardiography (MCE) to assess myocardial blood flow reserve  
277  
278 (MBFR). Informed consent was obtained for each patient. The study complied with the Declaration of Helsinki  
279  
280 and was approved by the local research ethics committee (H0102/78).  
281  
282

283 **2.2. CTA study:** CTA imaging was performed using a 64-channel CT scanner (GE Lightspeed VCT, GE Medical  
284  
285 Systems, USA). The mean heart rate during the scan was 64 beats/min. A low dose scout scan was performed  
286  
287 to define anatomic landmarks for the contrast-enhanced study. Calcium scoring and helical scan data was  
288  
289 performed on all patients using prospective ECG triggering at 75% of the R-R interval. Following this, a 20ml  
290  
291 bolus of contrast (Niopram 370®) at 6mls/sec was injected and the timing of peak contrast enhancement in the  
292  
293 aortic arch was used to determine the timing of scan acquisition. The contrast-enhanced scan used 80mls  
294  
295 contrast injected at 6 ml/s, followed by a 50ml at 6mls/sec saline flush, during a single expiration breath hold.  
296  
297  
298  
299  
300

301  
302  
303 The CTA scan parameters were: collimator 20mm, slice thickness 0.625mm; gantry rotation 350ms; helical  
304 acquisition using a pitch of 0.16; tube current 455-515 mA with ECG tube current modulation; tube voltage  
305 range 100-140kV; rotation time, 350ms. The estimated radiation dose per patient was 3.3mSv. Reconstructed  
306 CTA images were analysed on a dedicated 3-dimensional workstation (CardIQ Xpress, GE Medical Systems) with  
307 curved multiplanar reformation and short-axis cross sectional viewing techniques. We measured the amount of  
308 plaque present in the proximal, mid, and part of the distal sections, of the main vessel coronary artery tree.  
309 This decision was made because these segments have greater image quality regarding contrast:noise ratio,  
310 reduced observer variability, and contain the majority of clinically important plaque in the coronary tree (16,  
311 17). This included the left main stem (segment 1), the first 80mm of the left anterior descending (divided  
312 equally into segments 2 and 3), the first 30mm of the circumflex (segment 4) and the first 80mm of the right  
313 coronary artery (segments 5 and 6).

324  
325 **2.3. Aortic Valve Calcification Score (AVCS):** Amount of aortic valve calcification is correlated with the degree  
326 of aortic valve sclerosis applying multislice CT (18). For quantitative assessment of aortic valve calcification  
327 using CT with a detection threshold of 130H, the aortic valve Agatston score was derived. Calcification was  
328 attributed to the aortic valve if it was clearly part of the valve cusps. Supravalvular calcifications and  
329 calcifications of the coronary arteries including the ostia were removed by manual segmentation. The Agatston  
330 score was calculated by multiplying the lesion area by an attenuation factor derived from the maximal  
331 Hounsfield units within the area, as previously described (19). Figure 1 illustrates this analysis.

332  
333  
334  
335  
336  
337  
338  
339  
340 **2.4. Coronary artery plaque burden:** Total plaque length (TPL) was used as a surrogate measure of total  
341 atherosclerotic burden as described by Naya (20). Plaque length was measured as the distance (mm) from the  
342 proximal to the distal shoulder of each plaque. TPL was calculated for each patient by summing all the lengths  
343 for each subject. For each plaque, the degree of epicardial luminal narrowing was also assessed by quantifying  
344 the percentage diameter stenosis. This was calculated by dividing the minimal lumen diameter at each plaque  
345 by the nearest proximal normal artery diameter. The sum of all stenoses present divided by the number of  
346 stenosed plaques, determined the total mean stenosis per patient.

361  
362  
363 **2.5. Coronary Calcium Score:** 2.5mm slice thickness, non-overlapping images were reconstructed using filtered  
364  
365 back projection and a standard algorithm (GE). The total calcium burden in the coronary arteries was manually  
366  
367 measured by planimetry according to the scoring algorithm of Agatston (19).  
368  
369  
370  
371

372 **2.6. MCE study:** Patients underwent the MCE study having avoided all caffeine-containing products in the  
373  
374 previous 24 hours. Patients withheld beta-blockers, nitrates and calcium antagonists the day before, and on  
375  
376 the day of the test. MCE was performed using a commercial ultrasound machine iE33 (Philips Medical Systems)  
377  
378 and SonoVue (Bracco Research SA) as the contrast agent given as a constant infusion. Real-time images were  
379  
380 recorded within 3-4 minutes in the apical 4-, 2- and 3-chamber views with low-power settings at a mechanical  
381  
382 index of 0.1. The focus was set at the mitral valve level. SonoVue was initially started at 60 mL/h through a  
383  
384 peripheral vein cannula with the VueJect infusion syringe pump (Bracco Research, SA), which gently rotates  
385  
386 and maintains the contrast agent in a suspension. Thereafter, the rate was set between 48 and 60 mL/h to  
387  
388 maximize image quality with minimal attenuation. Once optimized, the machine settings were held constant  
389  
390 throughout each participant study. Flash-impulse imaging at a high mechanical index (1.0) was performed to  
391  
392 achieve complete myocardial bubble destruction, after which 10 end-systolic frames were recorded digitally in  
393  
394 each apical view. After the resting images were acquired, dipyridamole was infused at 0.56 mg/kg over a 4-  
395  
396 minute period. After an interval of 2 minutes, post-stress images were recorded within 3 to 4 minutes. This  
397  
398 entire sequence took 14 minutes. Quantitative MCE analysis was performed offline using QLab V7.0 (Q-  
399  
400 Laboratory, Philips Medical Systems) as previously described in detail (21). Briefly, quantitative assessment of  
401  
402 myocardial perfusion was performed for 10 consecutive end-systolic frames after microbubble destruction. A  
403  
404 region of interest was placed over the thickness of the myocardium. Plots of peak myocardial contrast intensity  
405  
406 (representing myocardial blood volume A, dB) versus pulsing intervals (representing time) were automatically  
407  
408 constructed to fit the monoexponential function conventional equation:  $y=A(1 - e^{-\beta t})$ . From these plots, the  
409  
410 slope of the replenishment curve was determined (representing myocardial blood velocity  $\beta$ , dB/s). Figure 2  
411  
412 illustrates this analysis technique. The product of A and  $\beta$  yielded baseline MBF (dB<sup>2</sup>/s) and post-dipyridamole  
413  
414 MBF (stress MBF, dB<sup>2</sup>/s), respectively. We calculated MBFR by the ratio of stress MBF (MBFs) to baseline MBF  
415  
416 (MBFb). MBFR was calculated by dividing the MBFs by MBFb of the same segment. Basal segments were not  
417  
418 included in the analysis because of contrast attenuation. The remaining 10 mid- and apical cardiac segments  
419  
420



421  
422  
423 were analyzed. A segment was not included in the analysis if there was artifact, inadequate microbubble  
424  
425 destruction, attenuation, or a wide variation in contrast intensity to minimize errors.  
426

427  
428 **2.7. Venous samples:** Peripheral venous samples for hs-CRP were taken at rest. Fasting glucose and lipid  
429  
430 profiles were from within the previous 3 months. All assays were performed in duplicate by a single observer,  
431  
432 blinded to the demographic data. Hs-CRP was determined with a particle-enhanced immunoassay, which has a  
433  
434 detection limit of 0.1mg/L and an inter-assay CV <10% (Roche Diagnostics, UK).  
435

436  
437 **2.8. Statistical Analysis:** Where appropriate, continuous variables were summarised using means, standard  
438  
439 deviations and/or 95% confidence intervals. Ordinal and dichotomous variables were summarised using  
440  
441 proportions or percentages. Indices of variance are bracketed after the respective value for central tendency.  
442  
443 Normality was assessed using a Shapiro-Wilk test and if deemed necessary, heavily skewed data were  
444  
445 transformed using a natural logarithmic transformation. General correlation was checked using a Pearson's  
446  
447 correlation coefficient, and for categorical data, a Spearman's rank correlation (rho) test was employed.  
448  
449 Statistical significance was tested using either a Student t-test for normally distributed continuous data or a  
450  
451 Mann-Whitney U-test for non-normal continuous data. Ordinal and dichotomous data were tested using a  
452  
453 Fischer exact test. Univariate regression was used initially to quantify the relationships between each of the  
454  
455 explanatory variables and the main outcome variable MBFR against AVCS. Based on the results of the  
456  
457 univariate regression, multivariable model building was performed using ordinary least-square regression and  
458  
459 the resulting models were tested for coefficient ( $\beta$ ) significance, model fit to data (adjusted  $R^2$ ) and residual  
460  
461 homoscedasticity and normality. If required, a leverage to squared residual plot was used to assess the effects  
462  
463 of either high leverage or outlying values on the regression coefficients. A likelihood ratio (LR) test was  
464  
465 employed to compare the fit of each successive iteration to the regression model. The level of significance was  
466  
467 set at  $P < 0.05$ . For CTA studies, 10 patients' scans (60 segments) were re-analysed by KN, and then again by two  
468  
469 additional separate observers who were level 2 accredited or above (KG, RB). All analyses were performed  
470  
471 using STATA™ version 12.0.  
472

### 473 **3. Results:**

474  
475  
476  
477  
478  
479  
480

481  
482  
483 Overall, our study included 183 participants whose baseline demographics are illustrated in Table 1. The mean  
484  
485 age of participants was 59.8( $\pm$ 9.6) years of whom 52.5% were male with a mean BMI of 27.2( $\pm$ 3.8) kg/m<sup>2</sup>. The  
486  
487 mean hs-CRP was 2.52( $\pm$ 3.86) mg/L, with 75 (41%) participants having elevated hs-CRP levels (defined as  
488  
489 >2mg/L).  
490  
491

492  
493 **3.1. Aortic valve analysis:** In those with aortic valve calcification, the mean aortic valve calcification score  
494  
495 (AVCS) was 68( $\pm$ 258) AU. In our cohort, the maximum AVCS was 2874 AU, and 72 (39%) had an AVCS of zero.  
496  
497 Due to the marked right skew present in AVCS, values were normalised using a natural logarithmic  
498  
499 transformation.  
500  
501

502  
503 **3.2. Coronary artery plaque morphology:** From the 1096 segments available for analysis, 1016(92%) were  
504  
505 interpretable. The total coronary tree length studied was 190mm plus the mean left main stem length (8mm+  
506  
507 7mm). Plaque was present in 113(62%) of patients. There were 384 plaques in total and 53(29%) of patients  
508  
509 had either one or two plaques present. The mean stenosis per patient was 3.1(0-22)% of whom 138(76%) had a  
510  
511 mean stenosis of <5%. Values for total plaque length (TPL) were right skewed with a median (IQRs) of 19.3 (8.9,  
512  
513 31.7) mm. The mean TPL was 15.6 mm, ranging from 0 to 132 mm. When present, the median coronary  
514  
515 calcification score was 43.5(IQR 10.5-152) AU. Total coronary calcification score was also markedly right-  
516  
517 skewed. Inter and intra-observer variability (kappa) for both aortic valve and coronary calcium scoring was 0.85  
518  
519 and 1.0, respectively.  
520  
521

522  
523 **3.3. Myocardial blood flow:** The mean MBFR was 2.20( $\pm$ 0.52), and 70 patients (38%) had an MBFR below 2.0.  
524  
525 The intra- and inter-observer variability's for MBFR were 7.7% and 8.2%, respectively. The minimum number of  
526  
527 analysable segments for baseline and stress was six for each, in keeping with previous published data (22).  
528  
529

530  
531 Table 2 shows the results of univariate analysis performed on all demographic parameters in addition to total  
532  
533 plaque length, coronary calcium score, hs-CRP and MBFR, in relation to aortic valve calcium score (AVCS). There  
534  
535 were significant positive correlations between increasing age, total plaque length, and hs-CRP with AVCS. There  
536  
537 was a significant negative correlation between MBFR, LDL and AVCS.  
538  
539  
540

541  
542  
543  
544  
545 Multivariate model analysis incorporated all univariate parameters with a P value <0.20, each as independent  
546 explanatory variables, using stepwise deletion from a fully saturated model. Each iteration was checked using a  
547 likelihood ratio test against the fully saturated null model. No significant interaction terms were identified. The  
548  
549 final regression equation is demonstrated in figure 3.  
550  
551

552  
553  
554 The tabulated values for regression coefficients ( $\beta$ ), 95% confidence intervals and P-values for each  $\beta$ , are listed  
555 in Table 3. Age, diabetes, BMI, MBFR, LDL and hs-CRP are all independent predictors of AVCS. Coronary calcium  
556 score and TPL were included separately during the model evolution due to strong collinearity and neither were  
557  
558 significant. As a result, the final model did not include either.  
559  
560  
561

562  
563  
564 Figure 3 shows the regression model used to predict values for aortic valve calcification score. In the model,  
565 increasing age, presence of diabetes, and hs-CRP are independent positive predictors of  $\ln(\text{AVCS})$ , whereas an  
566 increased MBFR, BMI, and LDL are negatively associated with  $\ln(\text{AVCS})$  ( $R^2=0.36$ ). From the model, an absolute  
567 change in the MBFR value by -1.0 results in an increase in AVCS by a multiple of 2.39AU.  
568  
569  
570  
571

#### 572 573 574 575 **4. Discussion:** 576

577  
578  
579 Coronary microvascular function as determined by measurement of myocardial blood flow reserve is an  
580 independent predictor of early CAVD. This effect is independent of the presence of coronary artery disease and  
581 also systemic inflammation. Importantly, although coronary artery disease is initially associated with CAVD,  
582 when MBFR is included in the model, coronary artery disease is no longer predictive.  
583  
584  
585

586  
587  
588 **4.1. AVCS and microvascular function:** Previous studies have reported CMD in CAVD, however there are  
589 several important differences with respect to our report. Banovic found that coronary flow reserve (CFR) using  
590 Doppler echocardiography of the left anterior descending coronary artery, is reduced in asymptomatic but  
591 haemodynamically significant moderate to severe AS with normal LV systolic function and unobstructed  
592 epicardial coronary arteries (13). Importantly, they found that CFR was an independent predictor of mortality  
593  
594  
595  
596  
597  
598  
599  
600

601  
602  
603 after multivariate analysis even after taking into account haemodynamic indices of AS. They proposed that  
604  
605 lower CFR values in this context were caused by the upstream effects of haemodynamically significant AS, such  
606  
607 as left ventricular hypertrophy and fibrosis, with consequent reduced capillary density. Similarly, Rajappan  
608  
609 assessed CMD in patients with moderate to severe AS with unobstructed coronary arteries but used positron  
610  
611 emission tomography to measure CMD (12). They found that parameters of AS severity such as aortic valve  
612  
613 area and haemodynamic load were associated with CMD. Neither of these studies determined whether  
614  
615 coronary artery disease was present even if mild. This is important because even the presence of mild early  
616  
617 coronary artery disease is associated with CMD. For instance, Wang showed that increasing coronary calcium  
618  
619 score in asymptomatic individuals is associated with reduced coronary perfusion reserve (15). In fact,  
620  
621 endothelial dysfunction in the context of chest pain with unobstructed coronary arteries is a predictor of future  
622  
623 coronary atherosclerosis (23).

624  
625  
626 There is relatively limited data with regards to the relationship between early CAVD (without  
627  
628 haemodynamically significant AS) and CMD. Bozbas assessed CFR in patients with aortic valve calcification  
629  
630 without significant aortic stenosis. Aortic valve calcification was assessed using echocardiography (14). The  
631  
632 authors found that mean CFR was 16% lower in the AVC group compared to control ( $p < 0.001$ ), and concluded  
633  
634 that CMD is present even during early CAVD. Multivariate analysis found that the presence of aortic valve  
635  
636 calcification was an independent predictor of CMD. However, although their patient cohort was asymptomatic,  
637  
638 they pointed out that their study had not excluded obstructive coronary artery disease.

639  
640  
641 Our study provides novel data for the following reasons. Firstly, early CAVD was diagnosed using CT, which is  
642  
643 more accurate than echocardiography in the assessment of aortic valve calcification (24). For example, one  
644  
645 group reported that CT had a greater sensitivity and detected 32% more patients than echocardiography in  
646  
647 their elderly screening cohort (24). The Agatston score for aortic valve calcification provides a much broader  
648  
649 range for quantitative scoring than the three point system used in Bozbas study. Finally, obstructive coronary  
650  
651 artery disease was excluded using CTCA whereas this was assumed from clinical history alone in previous  
652  
653 studies.

661  
662  
663 The role of microvascular dysfunction in relation to the development of CAVD is not yet clear. CMD has been  
664 shown to correlate closely with endothelial dysfunction (25) and peripheral endothelial dysfunction assessed  
665 using flow-mediated dilatation is also associated with aortic valve sclerosis. Therefore, when taken in  
666 conjunction with our results, this suggests a systemic process (26). The recent discovery that valve endothelial  
667 cells regulate the remodelling and integrity of the extracellular matrix within valve leaflets (27) may be  
668 important. It has been proposed that endothelial dysfunction allows inflammatory cytokine entry into valve  
669 leaflets which promotes mineralisation and ultimately leaflet calcification.  
670  
671  
672  
673  
674  
675  
676  
677

678 **4.2. AVCS and inflammation:** We found that the marker of systemic inflammation hs-CRP is independently  
679 associated with aortic valve calcification score and is consistent with other published data (28). Oxidative stress  
680 forms the initiating event of an inflammatory cascade which ultimately results in valvular calcification. Hs-CRP  
681 correlates strongly with oxidative stress and studies are underway regarding its use as a surveillance biomarker  
682 in the detection of atherosclerosis (5, 29). Furthermore, histopathology studies of explanted calcified aortic  
683 valves have found an abundance of leucocytes and macrophages (4). Our findings add to the literature in that  
684 CMD has a positive association with AVCS which is independent of and additive to the presence of systemic  
685 inflammation.  
686  
687  
688  
689  
690  
691  
692  
693  
694

695 **4.3. Other factors associated with early CAVD:** Our results indicated that Increasing age and presence of  
696 diabetes were positively associated with AVCS. Neither of these findings are novel. The strong link between age  
697 and valvular calcification is well established from epidemiology studies (3). Diabetes is a pro-inflammatory  
698 condition which promotes macrophage deposition and consequent calcification (1).  
699  
700  
701  
702  
703

704 Unexpectedly, in our analysis, increasing LDL was negatively associated with AVCS and is contrary to findings  
705 from previous studies (30, 31). Low-density lipoproteins have been implicated in the pathogenesis of CAVD.  
706 Extracellular lipid accumulation has been identified in explanted CAVD leaflets within the subendothelial layer  
707 with apolipoproteins, implying a plasma source (32). However, the role of LDL in the early stages of CAVD  
708 development is unknown especially given the failure of statin trials to slow AS progression (33). Importantly  
709 36% of this patient cohort were on statin therapy prior to recruitment, and therefore a proportion of the study  
710 population may have a history of chronically elevated LDL. Furthermore, recent reports have suggested that  
711  
712  
713  
714  
715  
716  
717  
718  
719  
720

lipid components other than LDL may be associated with AS progression and cardiovascular risk such as lipoprotein(a) (Lpa) and non-HDL, (34, 35).

Increasing BMI was negatively associated with AVCS in our analysis. This was unexpected as a high BMI is associated with both microvascular dysfunction and elevated systemic markers of inflammation, which promote calcification (36, 37). However, observational data showing increased survival rates in higher BMI patients presenting with acute coronary syndromes: the so-called obesity paradox, draws consideration of whether higher BMI confers protection against certain disease processes (38).

**4.4. Study Limitations:** The study was conducted at a single centre in the UK which means referral bias may have affected our sample population. Furthermore our participants consisted of patients referred for the investigation of chest pain, which is not representative of the general population. However, the recruitment of this patient population enabled CT-based radiological investigation which otherwise would not have been ethically possible, and is consistent with previous studies (2, 14).

## **5. Conclusion:**

Coronary microvascular function as determined by measurement of myocardial blood flow reserve is an independent predictor of early CAVD. This effect is independent of the presence of coronary artery disease and also systemic inflammation. Importantly, although coronary artery disease is initially associated with CAVD, when MBFR is included in the model, coronary artery disease is no longer predictive.

## REFERENCES

1. Alman AC, Kinney GL, Tracy RP, Maahs DM, Hokanson JE, Rewers MJ, et al. Prospective association between inflammatory markers and progression of coronary artery calcification in adults with and without type 1 diabetes. *Diabetes Care*. 2013;36(7):1967-73.
2. Nasir K, Katz R, Al-Mallah M, Takasu J, Shavelle DM, Carr JJ, et al. Relationship of aortic valve calcification with coronary artery calcium severity: the Multi-Ethnic Study of Atherosclerosis (MESA). *J Cardiovasc Comput Tomogr*. 2010;4(1):41-6.
3. Otto CM, Lind BK, Kitzman DW, Gersh BJ, Siscovick DS. Association of aortic-valve sclerosis with cardiovascular mortality and morbidity in the elderly. *NEJM*. 1999;341(3):142-7.
4. Mathieu P, Boulanger MC. Basic mechanisms of calcific aortic valve disease. *Can J Cardiol*. 2014;30(9):982-93.
5. Jeevanantham V, Singh N, Izuora K, D'Souza JP, Hsi DH. Correlation of high sensitivity C-reactive protein and calcific aortic valve disease. *Mayo Clin Proc*. 2007;82(2):171-4.
6. Gingham C, Florian A, Beladan C, Iancu M, Calin A, Popescu BA, et al. Calcific aortic valve disease and aortic atherosclerosis--two faces of the same disease? *Rom J Intern Med*. 2009;47(4):319-29.
7. Dweck MR, Khaw HJ, Sng GK, Luo EL, Baird A, Williams MC, et al. Aortic stenosis, atherosclerosis, and skeletal bone: is there a common link with calcification and inflammation? *Eur Heart J*. 2013;34(21):1567-74.
8. Johnson NP, Gould KL. Clinical evaluation of a new concept: resting myocardial perfusion heterogeneity quantified by markovian analysis of PET identifies coronary microvascular dysfunction and early atherosclerosis in 1,034 subjects. *J Nucl Med*. 2005;46(9):1427-37.
9. Bagi Z, Feher A, Cassuto J. Microvascular responsiveness in obesity: implications for therapeutic intervention. *Br J Pharmacol*. 2012;165(3):544-60.
10. Samim A, Nugent L, Mehta PK, Shufelt C, Bairey Merz CN. Treatment of angina and microvascular coronary dysfunction. *Curr Treat Options Cardiovasc Med*. 2010;12(4):355-64.
11. Eshtehardi P, McDaniel MC, Dhawan SS, Binongo JN, Krishnan SK, Golub L, et al. Effect of intensive atorvastatin therapy on coronary atherosclerosis progression, composition, arterial remodeling, and microvascular function. *J Invasive Cardiol*. 2012;24(10):522-9.
12. Rajappan K, Rimoldi OE, Dutka DP, Ariff B, Pennell DJ, Sheridan DJ, et al. Mechanisms of coronary microcirculatory dysfunction in patients with aortic stenosis and angiographically normal coronary arteries. *Circulation*. 2002;105(4):470-6.
13. Banovic M, Bosiljka VT, Voin B, Milan P, Ivana N, Dejana P, et al. Prognostic value of coronary flow reserve in asymptomatic moderate or severe aortic stenosis with preserved ejection fraction and nonobstructed coronary arteries. *Echocardiography*. 2014;31(4):428-33.
14. Bozbas H, Pirat B, Yildirim A, Simsek V, Sade E, Eroglu S, et al. Coronary flow reserve is impaired in patients with aortic valve calcification. *Atherosclerosis*. 2008;197(2):846-52.
15. Wang L, Jerosch-Herold M, Jacobs Jr DR, Shahar E, Detrano R, Folsom AR. Coronary Artery Calcification and Myocardial Perfusion in Asymptomatic Adults: The MESA (Multi-Ethnic Study of Atherosclerosis). *JACC*. 2006;48(5):1018-26.
16. Ferencik M, Nomura CH, Maurovich-Horvat P, Hoffmann U, Pena AJ, Cury RC, et al. Quantitative parameters of image quality in 64-slice computed tomography angiography of the coronary arteries. *Eur J Radiol*. 2006;57(3):373-9.
17. Hoffmann H, Frieler K, Hamm B, Dewey M. Intra- and interobserver variability in detection and assessment of calcified and noncalcified coronary artery plaques using 64-slice computed tomography: variability in coronary plaque measurement using MSCT. *Int J Cardiovasc Imaging*. 2008;24(7):735-42.
18. Koos R, Mahnken AH, Sinha AM, Wildberger JE, Hoffmann R, Kuhl HP. Aortic valve calcification as a marker for aortic stenosis severity: assessment on 16-MDCT. *AJR Am J Roentgenol*. 2004;183(6):1813-8.
19. Agatston AS, Janowitz WR, Hildner FJ, Zusmer NR, Viamonte M, Jr., Detrano R. Quantification of coronary artery calcium using ultrafast computed tomography. *JACC*. 1990;15(4):827-32.
20. Naya M, Murthy VL, Blankstein R, Sitek A, Hainer J, Foster C, et al. Quantitative relationship between the extent and morphology of coronary atherosclerotic plaque and downstream myocardial perfusion. *JACC*. 2011;58(17):1807-16.
21. Wei K, Ragosta M, Thorpe J, Coggins M, Moos S, Kaul S. Noninvasive quantification of coronary blood flow reserve in humans using myocardial contrast echocardiography. *Circulation*. 2001;103(21):2560-5.
22. Rana O BC, Kerr D, Coppini D, Zouwail S, Senior R, Begley J, Walker JJ, Greaves K. Acute Hypoglycaemia Decreases Myocardial Blood Flow Reserve in Patients With Type 1 Diabetes Mellitus and in Healthy Humans. *Circulation*. 2011;124:1548-56.

- 841  
842  
843 23. Bugiardini R, Manfrini O, Pizzi C, Fontana F, Morgagni G. Endothelial Function Predicts Future  
844 Development of Coronary Artery Disease: A Study of Women With Chest Pain and Normal Coronary  
845 Angiograms. *Circulation*. 2004;109(21):2518-23.
- 846 24. Owens DS, Plehn JF, Sigurdsson S, Probstfield JL, Launer LJ, Eiriksdottir G, et al. The comparable utility  
847 of computed tomography and echocardiography in the detection of early stage calcific aortic valve disease: an  
848 AGES-REYKJAVIK investigation. *JACC*. 2010;55(10s1):A71.E668-A71.E.
- 849 25. Pellegrino T, Storto G, Filardi PP, Sorrentino AR, Silvestro A, Petretta M, et al. Relationship between  
850 brachial artery flow-mediated dilation and coronary flow reserve in patients with peripheral artery disease. *J*  
851 *Nucl Med*. 2005;46(12):1997-2002.
- 852 26. Poggianti E, Venneri L, Chubuchny V, Jambrik Z, Baroncini LA, Picano E. Aortic valve sclerosis is  
853 associated with systemic endothelial dysfunction. *JACC*. 2003;41(1):136-41.
- 854 27. Gould ST, Srigunapalan S, Simmons CA, Anseth KS. Hemodynamic and cellular response feedback in  
855 calcific aortic valve disease. *Circ Res*. 2013;113(2):186-97.
- 856 28. Towler DA. Oxidation, inflammation, and aortic valve calcification peroxide paves an osteogenic path.  
857 *JACC*. 2008;52(10):851-4.
- 858 29. Ridker PM. High-sensitivity C-reactive protein: potential adjunct for global risk assessment in the  
859 primary prevention of cardiovascular disease. *Circulation*. 2001;103(13):1813-8.
- 860 30. Rajamannan NM. Mechanisms of aortic valve calcification: the LDL-density-radius theory: a translation  
861 from cell signaling to physiology. *Am J Physiol Heart Circ Physiol*. 2010;298(1):H5-H15.
- 862 31. Pohle K, Mäffert R, Ropers D, Moshage W, Stilianakis N, Daniel WG, et al. Progression of Aortic Valve  
863 Calcification: Association With Coronary Atherosclerosis and Cardiovascular Risk Factors. *Circulation*.  
864 2001;104(16):1927-32.
- 865 32. O'Brien KD, Reichenbach DD, Marcovina SM, Kuusisto J, Alpers CE, Otto CM. Apolipoproteins B, (a),  
866 and E accumulate in the morphologically early lesion of 'degenerative' valvular aortic stenosis. *Arterioscler*  
867 *Thromb Vasc Biol*. 1996;16(4):523-32.
- 868 33. Rossebø AB, Pedersen TR, Boman K, Brudi P, Chambers JB, Egstrup K, et al. Intensive Lipid Lowering  
869 with Simvastatin and Ezetimibe in Aortic Stenosis. *NEJM*. 2008;359(13):1343-56.
- 870 34. Capoulade R, Chan KL, Yeang C, Mathieu P, Bosse Y, Dumesnil JG, et al. Oxidized Phospholipids,  
871 Lipoprotein(a), and Progression of Calcific Aortic Valve Stenosis. *JACC*. 2015;66(11):1236-46.
- 872 35. Boekholdt S, Arsenault BJ, Mora S, et al. Association of ldl cholesterol, non-hdl cholesterol, and  
873 apolipoprotein b levels with risk of cardiovascular events among patients treated with statins: A meta-analysis.  
874 *JAMA*. 2012;307(12):1302-9.
- 875 36. Tona F, Serra R, Di Ascenzo L, Osto E, Scarda A, Fabris R, et al. Systemic inflammation is related to  
876 coronary microvascular dysfunction in obese patients without obstructive coronary disease. *Nutr Metab*  
877 *Cardiovasc Dis*. 2014;24(4):447-53.
- 878 37. Eroglu S, Sade LE, Bozbas H, Muderrisoglu H. Decreased coronary flow reserve in obese women. *Turk*  
879 *Kardiyol Dern Ars*. 2009;37(6):391-6.
- 880 38. Niedziela J, Hudzik B, Niedziela N, Gasior M, Gierlotka M, Wasilewski J, et al. The obesity paradox in  
881 acute coronary syndrome: a meta-analysis. *Eur J Epidemiol*. 2014;29(11):801-12.
- 882  
883  
884  
885  
886  
887  
888  
889  
890  
891  
892  
893  
894  
895  
896  
897  
898  
899  
900



901  
902  
903 **Table 1:** Baseline Demographics  
904

		All patients (n=183)
<b>Age in years; mean (SD)</b>		59.8 (9.6)
<b>Male sex (%)</b>		96 (52.4)
<b>Diabetes (%)</b>		18 (10.0)
<b>BMI (kg/m<sup>2</sup>) (SD)</b>		27.2 (3.8)
<b>Smoking History (%)</b>		
	<b>Non smoker</b>	100 (55)
	<b>Ex-smoker</b>	64 (35)
	<b>Current smoker</b>	19 (10)
<b>Hypertensive (%)</b>		71 (38.8)
<b>Family history (%)</b>		91 (49.7)
<b>Statin use (%)</b>		66 (36.0)

927  
928 BMI: Body mass index  
929  
930  
931  
932  
933  
934  
935  
936  
937  
938  
939  
940  
941  
942  
943  
944  
945  
946  
947  
948  
949  
950  
951  
952  
953  
954  
955  
956  
957  
958  
959  
960

**Table 2:** Univariate regression modelling of demographic variables, lipid profile and inflammation markers, coronary plaque parameters and microvascular function against aortic valve calcium score.

	$\beta$	95% CI	P-value
<b>Age (yrs)</b>	+0.07	+0.03, +0.10	0.01
<b>Male sex (Y/N)</b>	+0.05	-0.61, +0.71	0.08
<b>Diabetes (Y/N)</b>	+1.08	-0.11, +2.06	0.07
<b>BMI (kg/m<sup>2</sup>)</b>	-0.02	-0.12, +0.07	0.63
<b>Smoking category (Y/N)</b>	+0.31	-0.15, +0.77	0.19
<b>Hypertension (Y/N)</b>	+0.63	-0.02, +1.28	0.06
<b>Family history (Y/N)</b>	-0.36	-1.02, +0.30	0.29
<b>Statin use (Y/N)</b>	+0.63	-0.05, +1.30	0.07
<b>LDL (mmol/l)</b>	-0.45	-0.75, -0.15	0.003
<b>Triglyceride (mmol/l)</b>	+0.004	-0.33, +0.34	0.98
<b>Total plaque length (mm)</b>	+0.02	+0.01, +0.03	0.04
<b>Coronary calcium score (AU)</b>	+0.001	+0.001, +0.002	0.05
<b>hs-CRP (mg/L)</b>	+0.09	+0.01, +0.17	0.02
<b>MBFR</b>	-0.80	-1.41, -0.19	0.01

BMI: Body mass index, LDL: low-density lipoprotein, hs-CRP: high sensitivity C-reactive protein, MBFR:

myocardial blood flow reserve

**Table 3:** Multivariate regression modelling for predicting aortic valve calcification score using age, presence of diabetes, BMI, myocardial blood flow reserve, LDL, and hs-CRP

Variable	$\beta$	95% CI	P-value
Age (yrs)	+0.05	+0.02, +0.08	0.007
Diabetes (Y/N)	+1.03	+0.08, +1.98	0.033
BMI (kg/m <sup>2</sup> )	-0.11	-0.21, -0.01	0.033
MBFR	-0.87	-1.44, -0.30	0.003
LDL (mmol/l)	-0.32	-0.61, -0.03	0.029
hs-CRP (mg/L)	+0.09	+0.02, +0.16	0.010

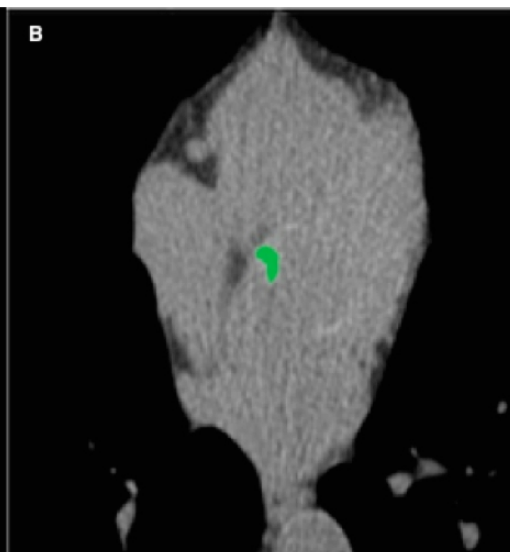
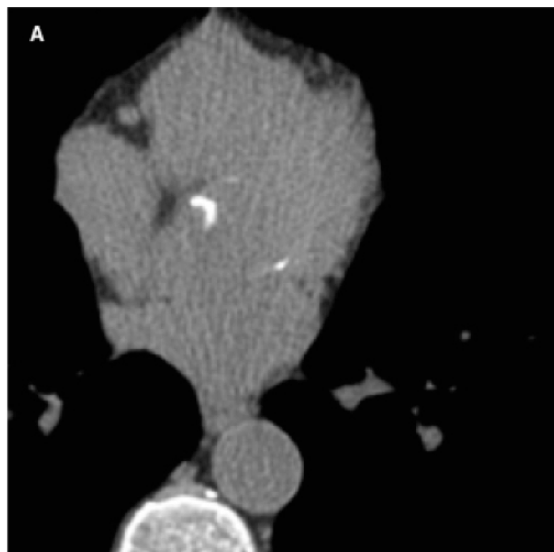
BMI: Body mass index, MBFR: Myocardial blood flow reserve, LDL: low-density lipoproteins, hs-CRP: high sensitivity C-reactive protein

1081  
1082  
1083 **Figure Captions:**  
1084  
1085  
1086

1087 **Figure 1.** Example of aortic valve calcium scoring using ECG-gated coronary CT images. Calcification of aortic  
1088 valve cusps detected on axial image (A). Imaging software detects regions within the aortic cusps with a density  
1089 threshold of greater than 130HU to derive calcium volume (B). Aortic valve calcium score is then calculated -  
1090 denoted in this case as 'U1' (C)  
1091  
1092  
1093

1094  
1095  
1096 **Figure 2.** Model used for quantitative analysis of myocardial segments. (A) Apical 4 chamber, (B) Apical 2  
1097 chamber, (C) Apical 3 chamber.  
1098  
1099  
1100

1101  
1102 **Figure 3.** Final model is described mathematically by  $\ln(\text{AVCS}) = 5.83 + (0.05 \times \text{age}) + (1.03 \times \text{diabetes}) - (0.11 \times$   
1103  $\text{BMI}) - (0.87 \times \text{MBFR}) - (0.32 \times \text{LDL}) + (0.09 \times \text{hs-CRP})$   
1104  
1105  
1106  
1107  
1108  
1109  
1110  
1111  
1112  
1113  
1114  
1115  
1116  
1117  
1118  
1119  
1120  
1121  
1122  
1123  
1124  
1125  
1126  
1127  
1128  
1129  
1130  
1131  
1132  
1133  
1134  
1135  
1136  
1137  
1138  
1139  
1140



**C**

Artery	Lesions	Volume [mm <sup>3</sup> ]	Equiv. Mass [mg]	Score
LM	0	0.0	0.00	0.0
LAD	0	0.0	0.00	0.0
CX	0	0.0	0.00	0.0
RCA	0	0.0	0.00	0.0
TOTAL	0	0.0	0.00	0.0
U1	2	155.6	31.76	189.1
U2	0	0.0	0.00	0.0

**Settings**  
Score Type: Agatston equivalent, Threshold: 130 HU (96.5 mg/cm<sup>2</sup> CaHA)  
Mass calibration factor: 0.743

